Bioorganic Chemistry 85 (2019) 558–567

Contents lists available at ScienceDirect

Bioorganic Chemistry

journal homepage: www.elsevier.com/locate/bioorg

Cytotoxic clerodane diterpenoids from the leaves of *Casearia kurzii*

Jun Ma[a], Xueyuan Yang[a], Qi Zhang[a], Xuke Zhang[a], Chunfeng Xie[a], Muhetaer Tuerhong[b], Jie Zhang[c], Da-Qing Jin[d], Dongho Lee[e], Jing Xu[a,*], Yasushi Ohizumi[f], Yuanqiang Guo[a,*]

[a] State Key Laboratory of Medicinal Chemical Biology, College of Pharmacy, and Tianjin Key Laboratory of Molecular Drug Research, Nankai University, Tianjin 300350, People's Republic of China
[b] College of Chemistry and Environmental Sciences, Laboratory of Xinjiang Native Medicinal and Edible Plant Resources Chemistry, Kashgar University, Kashgar 844000, People's Republic of China
[c] Key Laboratory for Green Processing of Chemical Engineering of Xinjiang Bingtuan, School of Chemistry and Chemical Engineering, Shihezi University, Shihezi 832003, People's Republic of China
[d] School of Medicine, Nankai University, Tianjin 300071, People's Republic of China
[e] Department of Biosystems and Biotechnology, College of Life Sciences and Biotechnology, Korea University, Seoul 02841, Republic of Korea
[f] Kansei Fukushi Research Institute, Tohoku Fukushi University, Sendai 989-3201, Japan

ARTICLE INFO

Keywords:
Clerodane diterpenoids
Cytotoxic activities
Casearia kurzii
Apoptosis
Cell cycle

ABSTRACT

A phytochemical investigation to obtain bioactive substances as lead compounds or agents for cancer led to the obtainment of six new clerodane diterpenoids, designated as kurzipenes A–F (**1–6**), from the leaves of *Casearia kurzii*. Their structures were elucidated on the basis of NMR spectroscopic data analysis and the absolute configurations were confirmed by the time-dependent density functional theory (TDDFT) electronic circular dichroism (ECD) calculations. The cytotoxic activities of compounds **1–6** were evaluated against human lung cancer A549 cell line, human cervical cancer Hela cell line, and human hepatocellular carcinoma HepG2 cell line. Most diterpenoids showed potent cytotoxicities against the three selected cancer cell lines. The preliminary mechanism studies revealed that the most active compound **2**, with an IC_{50} value of 5.3 μM against Hela cells, induced apoptosis and arrested the Hela cell cycle at the G0/G1 stage to exert cytotoxic effects.

1. Introduction

Natural products have been playing an important role in the research and development of new drugs and many new drugs are derived from natural products or natural product derivatives [1]. Among natural products, diterpenoids are a large group of compounds and have been found from many plants. The *Casearia* plants, belonging to the Flacourtiaceae plant family, consist of about 160 species and are distributed widely in tropical Africa, Asia, northwest Australia, and South America [2]. Some species of this genus have been used as folk medicines for multiple pathologic symptoms [3]. Recent phytochemical investigations have also shown the genus *Casearia* to be a rich source of diterpenoids, especially clerodane diterpenoids [3–15]. These reported diterpenoids showed various biological effects, such as antimalarial, cytotoxic, antifungal, antimicrobial, and DNA-modifying activities [3].

The species *Casearia kurzii* C. B. Clarke, is a small tree growing mainly in Yunnan Province of China, India, and the north of Burma [2]. There are no records on its traditionally medicinal purposes in Chinese medical books and no phytochemical reports on its chemical constituents. Considering the applications of some *Casearia* species as folk medicines and the discovery of bioactive components from some *Casearia* plants [3], the chemical constituents of the leaves of *C. kurzii* were investigated during our search for bioactive substances from plants [16,17]. This investigation led to the isolation of six new clerodane diterpenoids, designated as kurzipenes A–F (**1–6**) (Fig. 1). Their structures were elucidated on the basis of 1D and 2D NMR spectroscopic data analysis, and the absolute configurations of **1–6** were established by comparing their experimental electronic circular dichroism (ECD) spectra with those calculated by the time-dependent density functional theory (TDDFT) method. All of the isolates were evaluated for their cytotoxic activities against three tumor cell lines including human lung cancer A549 cells, human cervical cancer Hela cells, and human hepatocellular carcinoma HepG2 cells. The most active compound **2** was selected to investigate the possible action mechanism. Herein, the isolation, structural elucidation, and cytotoxic effects of these new compounds as well as the cytotoxic mechanism are described.

* Corresponding authors.
E-mail addresses: xujing611@nankai.edu.cn (J. Xu), victgyq@nankai.edu.cn (Y. Guo).

https://doi.org/10.1016/j.bioorg.2019.01.048
Received 19 May 2018; Received in revised form 22 January 2019; Accepted 24 January 2019
Available online 02 February 2019
0045-2068/

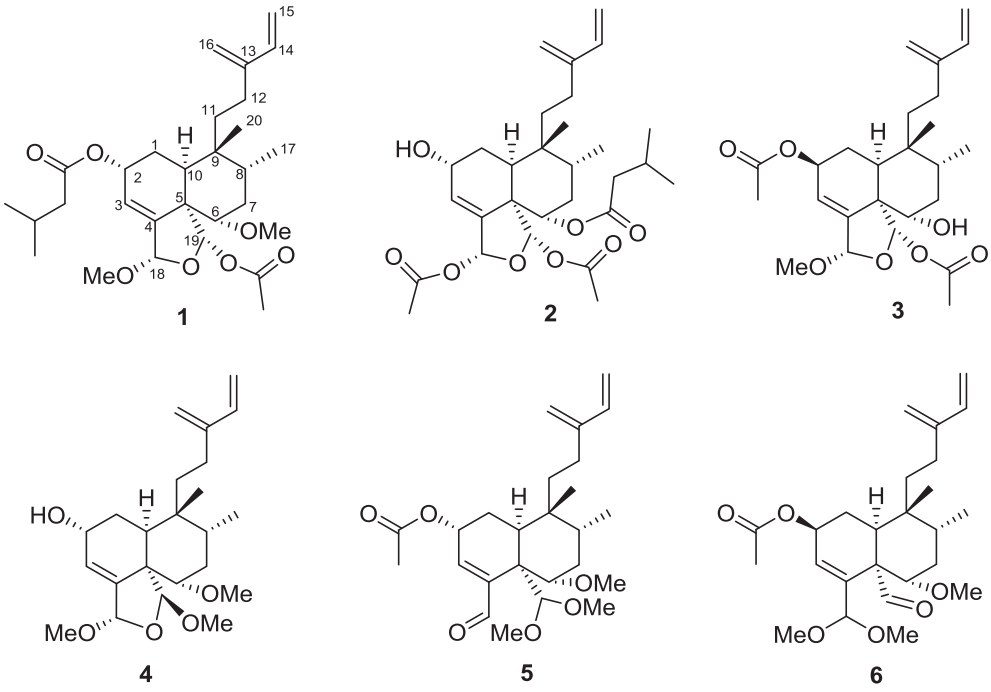

Fig. 1. Structures of compounds **1–6** from *C. kurzii*.

2. Experimental

2.1. General experimental procedures

Optical rotations were recorded on an InsMark IP120 automatic polarimeter (InsMark Instrument Co., Ltd., Shanghai, People's Republic of China). ECD spectra were obtained on a JASCO J-715CD spectrometer (JASCO Corporation, Tokyo, Japan). Infrared (IR) spectra were taken on a Bruker Tensor II FT-IR spectrometer (Bruker Optics, Ettlingen, Germany). 1D and 2D NMR experiments were performed on a Bruker AV 400 instrument (Bruker, Switzerland, 100 MHz for ^{13}C and 400 MHz for ^{1}H) with TMS as an internal reference at room temperature. HRESIMS were recorded by IonSpec 7.0 T FTICR MS (IonSpec Co., Ltd., Lake Forest, CA, USA) or ACQUITY UPLC I-Class SYNAPT G2-Si HDMS (Waters Corp. UK). HPLC separations were conducted on a CXTH system, equipped with a Shodex RI-102 detector (Showa Denko Co., Ltd., Tokyo, Japan) and a YMC-pack ODS-AM (20 × 250 mm) column (YMC Co., Ltd., Kyoto, Japan). Medium pressure liquid chromatography (MPLC) was run on a P0100 pump with an ultraviolet (UV) detector (Huideyi Co., Beijing, People's Republic of China) and a column (40 × 400 mm) filled by octadecylsilyl (ODS, 50 μm, YMC Co., Ltd.). Silica gel (200–300 mesh) used for column chromatography was purchased from Qingdao Haiyang Chemical Group Co., Ltd. (Qingdao, People's Republic of China). Chemical reagents (analytical grade) and biological reagents were provided by Tianjin Chemical Reagent Co. (Tianjin, People's Republic of China) and Sigma Co., respectively. A549, Hela, and HepG2 cell lines were from Shanghai Institutes for Biological Sciences, Chinese Academy of Sciences (Shanghai, People's Republic of China).

2.2. Plant material

The leaves of *C. kurzii* were collected in May 2015 from Xishuangbanna, Yunnan Province, People's Republic of China. The botanical identification was made by one of the authors (Y. Guo), and a voucher specimen (No. 20150525X) was deposited at the laboratory of bioactive substance and function of natural medicines, Nankai University, People's Republic of China.

2.3. Extraction and isolation

The air-dried leaves of *C. kurzii* (14.0 kg) were extracted with MeOH (3 × 162 L) under reflux. The solvent was evaporated to afford a crude extract (3.1 kg). This extract was suspended in H_2O (3.1 L) and partitioned with petroleum ether and ethyl acetate successively to give a petroleum ether-soluble portion (540.0 g) and an ethyl acetate-soluble portion (423.0 g). The EtOAc-soluble part (423.0 g) was subjected to silica gel column chromatography (silica gel, 1350 g; column, 10 × 50 cm), using a gradient of acetone in petroleum ether (100: 2, 100: 4, 100: 7, 100: 11, 100: 16, 100: 24, and 100: 35, 21 L for each gradient elution), to give eight fractions (F_1–F_8) based on TLC analysis. Fraction F_4 was separated by MPLC over ODS eluting with a step gradient from 67 to 95% MeOH in H_2O to afford seven subfractions ($F_{4\text{-}1}$–$F_{4\text{-}7}$). The following procedure was the purification of these subfractions. Using the preparative HPLC, compound **1** (t_R = 55 min, 3.6 mg) was obtained from $F_{4\text{-}5}$ (84% MeOH in H_2O), compound **3** (t_R = 62 min, 5.0 mg) was isolated from $F_{4\text{-}3}$ (76% MeOH in H_2O), and compound **6** (t_R = 47 min, 8.3 mg) was from $F_{4\text{-}4}$ (83% MeOH in H_2O). Fraction F_6 was fractionated with the same MPLC eluting with a step gradient from 66 to 93% MeOH in H_2O to afford five subfractions ($F_{6\text{-}1}$–$F_{6\text{-}5}$). Compound **2** (t_R = 46 min, 11.0 mg) was isolated from the subfraction $F_{6\text{-}3}$ by preparative HPLC (82% MeOH in H_2O) and compound **4** (t_R = 45 min, 6.3 mg) was obtained from $F_{6\text{-}2}$ (78% MeOH in H_2O). Using the same MPLC system as for the above fractions, F_5 provided subfractions $F_{5\text{-}1}$–$F_{5\text{-}6}$. The subsequent purification of $F_{5\text{-}4}$ by the same HPLC system (85% MeOH in H_2O) resulted in the isolation of compound **5** (t_R = 37 min, 9.6 mg).

2.3.1. Kurzipene A (*1*)

Colorless oil; $[\alpha]_D^{21}$ +32.4 (c = 0.29, CH_2Cl_2); ECD (CH_3CN) 201.3 ($\Delta\varepsilon$ 8.8) nm; IR (film) ν_{max} cm^{-1}: 2960, 2881, 1749, 1463, 1372, 1222, 1106, 946, 892, 734; ^{13}C NMR (100 MHz, $CDCl_3$) and ^{1}H NMR (400 MHz, $CDCl_3$) data, see Tables 1 and 2; ESIMS m/z 527 $[M+Na]^+$; HRESIMS m/z 527.2985 $[M+Na]^+$, calcd for $C_{29}H_{44}NaO_7$, 527.2985.

2.3.2. Kurzipene B (*2*)

Colorless oil; $[\alpha]_D^{20}$ +6.9 (c = 0.29, CH_2Cl_2); ECD (CH_3CN) 199.3 ($\Delta\varepsilon$ 10.2), 220.3 ($\Delta\varepsilon$ −4.1) nm; IR (film) ν_{max} cm^{-1}: 3479, 2980, 2884,

Table 1
^{13}C NMR data for compounds **1–6** (100 MHz, δ in ppm).

Position		1		2		3		4		5		6	
1		27.2	CH_2	27.9	CH_2	26.9	CH_2	29.8	CH_2	25.7	CH_2	26.0	CH_2
2		66.2	CH	63.8	CH	71.0	CH	63.6	CH	65.7	CH	70.8	CH
3		120.9	CH	126.4	CH	126.7	CH	123.4	CH	139.1	CH	128.3	CH
4		147.0	C	145.2	C	145.1	C	147.0	C	144.1	C	142.2	C
5		52.9	C	52.2	C	51.9	C	51.4	C	56.7	C	56.4	C
6		82.3	CH	73.8	CH	72.6	CH	84.0	CH	82.1	CH	82.7	CH
7		31.1	CH_2	33.1	CH_2	35.9	CH_2	31.8	CH_2	31.8	CH_2	32.1	CH_2
8		36.9	CH	36.7	CH	41.9	CH	37.1	CH	35.9	CH	42.9	CH
9		37.4	C	37.4	C	38.1	C	37.9	C	38.2	C	38.7	C
10		36.3	CH	36.2	CH	36.2	CH	39.0	CH	38.7	CH	35.9	CH
11		27.8	CH_2	29.5	CH_2	27.2	CH_2	28.8	CH_2	31.6	CH_2	31.3	CH_2
12		23.7	CH_2	23.8	CH_2	23.8	CH_2	25.1	CH_2	24.0	CH_2	23.5	CH_2
13		145.2	C	142.5	C	145.0	C	146.8	C	146.5	C	146.4	C
14		140.5	CH	140.3	CH	140.3	CH	139.5	CH	124.6	CH	139.1	CH
15		112.2	CH_2	112.6	CH_2	112.5	CH_2	113.1	CH_2	113.0	CH_2	113.0	CH_2
16		115.5	CH_2	115.4	CH_2	115.6	CH_2	115.1	CH_2	116.0	CH_2	115.8	CH_2
17		15.9	CH_3	15.6	CH_3	15.7	CH_3	15.8	CH_3	15.6	CH_3	15.5	CH_3
18		104.4	CH	95.3	CH	103.7	CH	102.1	CH	201.7	CH	103.1	CH
19		98.0	CH	98.3	CH	98.6	CH	111.7	CH	103.8	CH	201.6	CH
20		25.6	CH_3	25.5	CH_3	25.6	CH_3	26.5	CH_3	26.2	CH_3	26.3	CH_3
OR-2[a]	1	172.8	C			170.9	C			170.7	C	170.6	C
	2	43.7	CH_2			21.2	CH_3			21.4	CH_3	21.3	CH_3
	3	26.0	CH										
	4	22.4	CH_3										
	5	22.5	CH_3										
OCH_3-6[a]	1	57.5	CH_3	172.5	C			58.4	CH_3	57.1	CH_3	56.9	CH_3
	2			43.7	CH_2								
	3			25.5	CH								
	4			22.3	CH_3								
	5			22.4	CH_3								
OR-18[a]	1	55.5	CH_3	170.2	C							53.6	CH_3
	2			21.3	CH_3	56.2	CH_3	56.1	CH_3			54.7	CH_3
OR-19[a]	1	170.2	C	170.0	C	169.9	C			54.4	CH_3		
	2	21.8	CH_3	21.7	CH_3	21.6	CH_3	58.1	CH_3	55.0	CH_3		

[a] A number with a superscript indicates the location of the substituent group in the parent skeleton.

1734, 1373, 1223, 1100, 919, 895, 734; ^{13}C NMR (100 MHz, $CDCl_3$) and ^1H NMR (400 MHz, $CDCl_3$) data, see Tables 1 and 2; ESIMS *m/z* 541 $[M+Na]^+$; HRESIMS *m/z* 541.2776 $[M+Na]^+$, calcd for $C_{29}H_{42}NaO_8$, 541.2778.

2.3.3. Kurzipene C (3)

Colorless oil; $[\alpha]_D^{19}$ −98.5 (*c* = 0.27, CH_2Cl_2); ECD (CH_3CN) 201.7 ($\Delta\varepsilon$ −8.6) nm; IR (film) ν_{max} cm^{-1}: 3452, 2967, 2884, 1736, 1371, 1171, 1099, 949, 896, 734; ^{13}C NMR (100 MHz, $CDCl_3$) and ^1H NMR (400 MHz, $CDCl_3$) data, see Tables 1 and 2; ESIMS *m/z* 471 $[M+Na]^+$; HRESIMS *m/z* 471.2358 $[M+Na]^+$, calcd for $C_{25}H_{36}NaO_7$, 471.2359.

2.3.4. Kurzipene D (4)

Colorless oil; $[\alpha]_D^{20}$ +10.7 (*c* = 0.30, CH_2Cl_2); ECD (CH_3CN) 199.8 ($\Delta\varepsilon$ 5.0), 222.5 ($\Delta\varepsilon$ −0.6), 238.6 ($\Delta\varepsilon$ 0.3) nm; IR (film) ν_{max} cm^{-1}: 3448, 2980, 1717, 1458, 1378, 1107, 1013, 968, 894, 733; ^{13}C NMR (100 MHz, $CDCl_3$) and ^1H NMR (400 MHz, $CDCl_3$) data, see Tables 1 and 2; ESIMS *m/z* 415 $[M+Na]^+$; HRESIMS *m/z* 415.2460 $[M+Na]^+$, calcd for $C_{23}H_{36}NaO_5$, 415.2460.

2.3.5. Kurzipene E (5)

Colorless oil; $[\alpha]_D^{20}$ −8.2 (*c* = 0.34, CH_2Cl_2); ECD (CH_3CN) 190.0 ($\Delta\varepsilon$ 5.4), 215.3 ($\Delta\varepsilon$ 0.2), 231.1 ($\Delta\varepsilon$ 1.0), 257.3 ($\Delta\varepsilon$ −0.8), 280.5 ($\Delta\varepsilon$ −0.4), 306.3 ($\Delta\varepsilon$ −0.6) nm; IR (film) ν_{max} cm^{-1}: 2980, 2885, 1729, 1451, 1374, 1236, 1170, 1018, 956, 734; ^{13}C NMR (100 MHz, $CDCl_3$) and ^1H NMR (400 MHz, $CDCl_3$) data, see Tables 1 and 2. ESIMS *m/z* 457 $[M+Na]^+$; HRESIMS *m/z* 457.2562 $[M+Na]^+$, calcd for $C_{25}H_{38}NaO_6$, 457.2566.

2.3.6. Kurzipene F (6)

Colorless oil; $[\alpha]_D^{19}$ −28.1 (*c* = 0.29, CH_2Cl_2); ECD (CH_3CN) 190.0 ($\Delta\varepsilon$ 1.0), 214.0 ($\Delta\varepsilon$ −2.2), 237.4 ($\Delta\varepsilon$ −0.6), 252.8 ($\Delta\varepsilon$ −1.0), 276.1 ($\Delta\varepsilon$ −0.3), 302.4 ($\Delta\varepsilon$ −0.4) nm; IR (film) ν_{max} cm^{-1}: 2980, 2884, 1731, 1452, 1375, 1239, 1076, 952, 881, 734; ^{13}C NMR (100 MHz, $CDCl_3$) and ^1H NMR (400 MHz, $CDCl_3$) data, see Tables 1 and 2; ESIMS *m/z* 473 $[M-H+OH+Na]^+$; HRESIMS *m/z* 473.2518 $[M-H+OH+Na]^+$, calcd for $C_{25}H_{38}NaO_7$, 473.2515.

2.4. Computational method

The calculated ECD spectra of new compounds were performed as previously reported [18,19]. According to the conformation of every compound deduced from NOESY spectra and Chem3D modeling, systematic conformational searches were performed firstly using MOE software and appropriate conformers were selected for geometry optimizations. Geometry optimizations and re-optimizations on the B3LYP/6-31 + G(d,p) level were performed by Gaussian 09 package [20]. The TDDFT ECD calculations for the optimized conformers were carried out at the CAM-B3LYP/SVP level with a CPCM solvent model in acetonitrile, and the calculated ECD spectra of different conformers were simulated with a half bandwidth of ~0.4 eV. The ECD curves were extracted by SpecDis 1.62 software [21]. The overall ECD curves of all the compounds were weighted by Boltzmann distribution after UV correction.

2.5. Cytotoxic activity assay

The cytotoxic activities were evaluated using MTT assay. Cells were cultured in RPMI-1640 (A549 and Hela cells) or DMEM (HepG2 cells) medium supplemented with 10% (v/v) fetal bovine serum and 100 U/mL penicillin/streptomycin under a water-saturated atmosphere of 95% air and 5% CO_2. After reaching approximate 80% confluence, the cells

Table 2
^{1}H NMR data for compounds **1–6** (400 MHz, δ in ppm, J in Hz).

Position		1	2	3	4	5	6
1α		1.97 m	1.55 m	2.17 m	1.91 m	1.86 m	2.14 m
1β		1.89 m	1.28 m	1.73 m	1.25 m	1.66 m	1.50 m
2		5.47 brs	4.44 brs	5.56 t (8.3)	4.34 brs	5.38 t (4.3)	5.52 t (8.6)
3		6.00 d (4.1)	6.00 d (4.1)	6.07 brs	6.01 d (3.8)	6.35 brs	6.17 brs
6		3.29 dd (4.4, 11.6)	4.98 dd (5.2, 11.3)	4.09 dd (4.5, 12.1)	3.26 dd (4.4, 12.3)	3.38 dd (4.3, 12.6)	3.56 dd (5.0, 11.2)
7α		1.81 m	1.70 m	1.76 m	2.07 m	1.96 m	1.95 m
7β		1.50 m	1.63 m	1.67 m	1.63 m	1.66 m	1.63 m
8		1.70 m	1.90 m	2.20 m	1.73 m	1.65 m	2.36 d (13.4)
10		2.31[b]	2.35 dd (4.1, 12.9)	1.87[b]	1.90[b]	2.48 dd (2.8, 13.9)	1.66[b]
11		1.48 m	2.09 m	1.47 m	2.13 m	2.09 m	1.45 m
		1.26 m	1.98 m	1.20 m	1.32 m	1.10 m	1.16 m
12		2.08 m	2.11 m	2.04 m	2.14 m	2.06 m	2.00 m
14		6.43 dd (10.8, 17.5)	6.43 dd (10.8, 17.6)	6.42 dd (10.7, 17.8)	6.39 dd (10.0, 17.5)	6.35 dd (10.9, 17.4)	6.34 dd (11.0, 17.7)
15		5.17 d (17.5)	5.22 d (17.6)	5.22 d (17.8)	5.23 d (17.5)	5.22 d (17.4)	5.22 d (17.7)
		5.02 d (10.8)	5.04 d (10.8)	5.03 d (10.7)	5.06 d (10.0)	5.05 d (10.9)	5.04 d (11.0)
16		5.05 s	5.06 s	5.05 s	5.04 s	5.03 s	5.01 s
		4.94 s	4.94 s	4.93 s		5.00 s	4.99 s
17		0.94 d (6.7)	0.92 d (7.0)	0.93 d (6.8)	0.92 d (6.6)	0.89 d (6.0)	0.89 d (6.0)
18		5.42 s	6.52 s	5.24 s	5.52 s	9.90 s	4.88 s
19		6.41 s	6.54 s	6.51 s	4.86 s	4.85 s	9.94 s
20		0.91 s	0.99 s	0.95 s	1.00 s	0.96 s	0.98 s
OR-2[a]	2	2.25 m		2.09 s		2.08 s	2.07 s
	3	2.13 m					
	4	1.00 d (7.1)					
	5	1.00 d (7.1)					
OCH_3-6[a]	2	3.29 s	2.20 m		3.32 s	3.36 s	3.39 s
	3		1.91 m				
	4		0.94 d (7.1)				
	5		0.94 d (7.1)				
OR-18[a]	1	3.40 s		3.49 s	3.52 s		3.17 and 3.33 (s)
	2		2.07 s				
OR-19[a]	1					3.23 s	
	2	1.86 s	1.90 s	1.85 s	3.43 s	3.32 s	

[a] A number with a superscript indicates the location of the substituent group in the parent skeleton.
[b] Signals are in overlapped regions of the spectra, and the multiplicities could not be discerned.

were harvested and seeded in 96-well plates (1×10^4 cells/well) and allowed to adhere for 24 h at 37 °C. Then, the cells were treated with the test samples dissolved in DMSO at different concentrations, including the positive and the negative controls. Etoposide was used as a positive control. After a continuous incubation for 48 h, 20 μL MTT solution (5 mg/mL, Solarbio, Beijing, People's Republic of China) were added in each well for 4 h. Then, the medium was replaced with 150 μL DMSO and the absorbance was measured at 492 nm using microplate reader (Thermo Fisher Scientific Inc. America). The experiments were performed in triplicate, and the IC_{50} value was defined as the concentration of the compounds that inhibited cell proliferation by 50%.

2.6. Apoptosis analysis by flow cytometry

Cell apoptosis was analyzed by flow cytometry using Annexin V-FITC Apoptosis Detection Kit (Beyotime, Shanghai, People's Republic of China) according to the manufacturer's instruction. Briefly, Hela cells were treated with various concentrations (2.7, 8, and 24 μM) of the selected compound. After an incubation of 48 h, the cells were washed twice with PBS and resuspended in the binding buffer (Beyotime, Shanghai, People's Republic of China). This suspension was incubated for 20 min at room temperature in the dark after adding 5 μL Annexin V-FITC and 10 μL PI. Then, cell apoptosis was examined by BD LSRFortessa flow cytometry (BD Biosciences). The cell apoptosis data were obtained with FLOWJO flow cytometry analysis software (FLOWJO LLC, USA).

2.7. Cell cycle analysis

Flow cytometric analysis was performed to evaluate the distribution of cell cycle. Hela cells in exponential growth phase were seeded in 24 well plate and treated with different concentrations of selected compound (1.5, 5, and 15 μM). After an exposure to the test samples for 48 h, the cells were harvested, washed with PBS twice, and fixed in 70% ice-cold ethanol at 4 °C overnight. Then, the cells were washed with PBS twice and treated with propidium iodide staining buffer containing RNase (Beyotime, Shanghai, People's Republic of China) for 30 min at 37 °C in the dark, followed immediately by cellar DNA analysis using BDLSR Fortessa flow cytometry. Data were processed using ModFit LT Software.

3. Results and discussion

3.1. Structure elucidation

The ethyl acetate-soluble part of the methanol extract of the leaves of *C. kurzii* was fractionated by column chromatography and purified by HPLC to afford six new diterpenoids (**1–6**).

Compound **1** was obtained as a colorless oil. Its molecular formula was determined as $C_{29}H_{44}O_7$ by HRESIMS which displayed a pseudo molecular ion peak at m/z 527.2985 $[M+Na]^+$ (calcd for $C_{29}H_{44}NaO_7$, 527.2985). The ^{1}H NMR spectrum of **1** exhibited signals for six olefinic protons [δ_H 6.00 (1H, d, J = 4.1), 6.43 (1H, dd, J = 17.5, 10.8 Hz), 5.17 (1H, d, J = 17.5 Hz), 5.02 (1H, d, J = 10.8 Hz), and 5.05 and 4.94 (each 1H, s, H_2-16)], four oxygenated methine protons [δ_H 5.47 (1H, brs), 3.29 (1H, dd J= 4.4, 11.6 Hz), 5.42 (1H, s), and 6.41 (1H, s)], and five methyl groups [δ_H 0.94 (d, J = 6.7 Hz), 0.91 (s), 1.00 × 2 (d, J = 7.1 Hz), and 1.86 (s)]. The ^{13}C NMR spectrum of **1** showed 29 carbon resonances (Table 1), of which the signals (δ_C 170.2, 21.8, 57.5, and 55.5) were indicative of one acetyloxy and two methoxy groups. In addition to these substituent groups, an isovaleryloxy moiety was deduced and defined from the observation of the following carbon signals

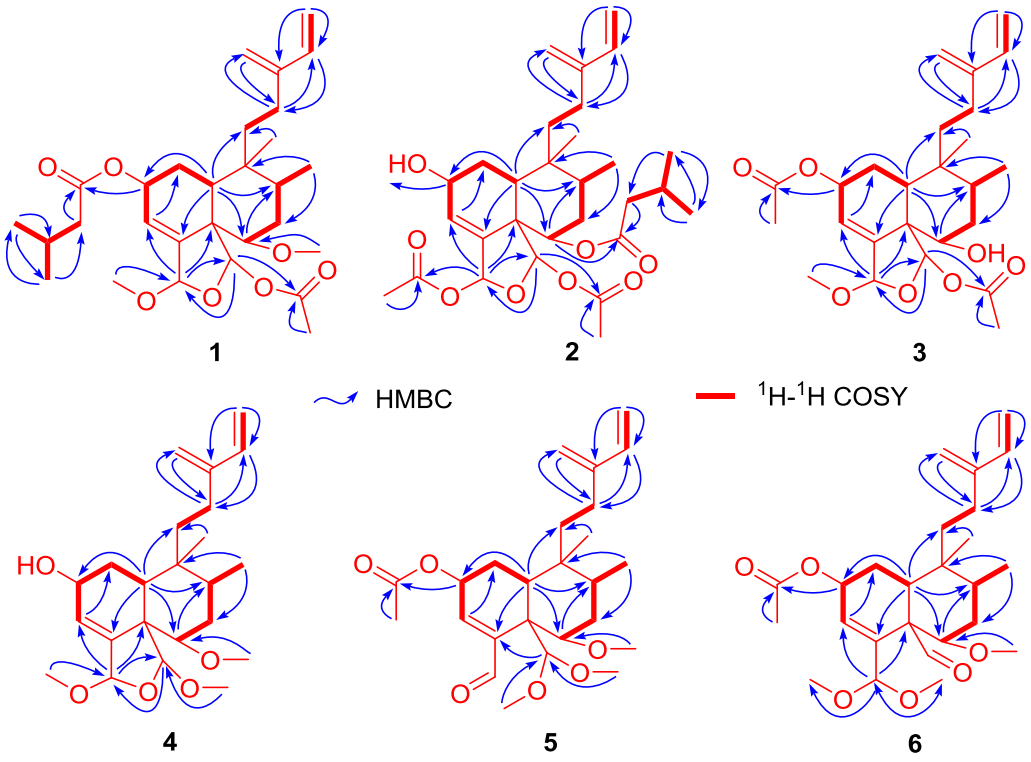

Fig. 2. ^{1}H-^{1}H COSY and selected HMBC correlations of compounds **1–6**.

(δ_C 172.8, 43.7, 26.0, 22.5, and 22.4) and the corresponding methyl, methylene, and methine proton signals (Table 2). Apart from these carbon signals for the substituent groups, additional 20 resonances for the skeleton were displayed in the ^{13}C NMR spectrum, including six olefinic and two acetal carbons based on the DEPT and HMQC spectra. These 20 typical skeletal carbons, especially the two acetal (δ_C 104.4 and 98.0) and four olefinic carbons (δ_C 145.2, 140.5, 115.5, and 112.2) forming two terminal double bonds, implied that compound **1** should be a clerodane-type diterpenoid according to those diterpenoids reported previously from the genus *Casearia* [22–25]. This structure of clerodane-type diterpenoid was elucidated and confirmed as shown in Fig. 2 by HMBC and ^{1}H-^{1}H COSY experiments. By analyzing 2D NMR spectra, the olefinic, acetal, and oxygenated carbon signals at δ_C 120.9 (C-3), 147.0 (C-4), 145.2 (C-13), 140.5 (C-14), 112.2 (C-15), 115.5 (C-16), 104.4 (C-18), 98.0 (C-19), 66.2 (C-2), and 82.3 (C-6) were assigned, and detailed analysis of the 1D and 2D NMR data allowed the other proton and carbon signals to be attributed. The positions of the isovaleryloxy, methoxy, and acetyloxy groups were deduced from the HMBC spectrum. The long-range coupling of the proton signal at δ_H 5.47 (H-2) with the carbonyl signal at δ_C 172.8 demonstrated that the isovaleryloxy moiety was attached at C-2. Similarly, the acetyloxy group was inferred to be attached at C-19 by the HMBC correlations of H-19 with the corresponding carbonyl carbons of the acetyloxy group. The two methoxy groups left were attributed to C-18 and C-6 from the long-range couplings of H-18 and H-6 to the corresponding methoxy carbons. All of the above spectroscopic data analysis disclosed a planar structure for **1** as depicted in Fig. 2.

The configuration of **1** was determined from the NOESY spectrum, Chem3D modeling, and ECD calculations. NOESY interactions observed for H-1β/H-8, H-8/H-6, H-1β/H-6, H-18/H-19, H-19/H$_2$-11, H-19/H-7α, H-7α/H$_2$-11, H-7α/H$_3$-17, H-10/H$_2$-11, and H-1α/H$_3$-20, together with Chem3D modeling, revealed a conformation for compound **1** as shown in Fig. 3. According to this molecular arrangement of **1**, two six-membered rings A and B were *cis*-fused with H-10 and C-19 both on the α-side, ring A presented a twisted chair conformation with the C-2 isovaleryloxy group in an α-position, ring B had a normal chair conformation with H-6 and Me-20 both β-oriented and Me-17 α-oriented, and ring C adopted an envelope conformation with H-18 and H-19 both in β-positions. The relative configuration of **1** was therefore designated as illustrated in Fig. 3. The absolute configuration of **1** was established via comparison of experimental and calculated ECD data, a tool to assign the absolute configuration of natural products [18,19]. Through systematic conformational search and geometry optimizations by MOE and Gaussian 09 [20], the ECD calculations at the B3LYP/SVP level with the CPCM model in acetonitrile were performed. The calculated ECD spectrum of **1** (Fig. 4A) matched the experimental data closely, which suggested an absolute configuration of 2*R*, 5*S*, 6*S*, 8*R*, 9*R*, 10*S*, 18*S*, and 19*S*. The structure of **1** was therefore elucidated as shown, and the compound was named kurzipene A.

Compound **2** was also obtained as a colorless oil. Its HRESIMS showed a molecular ion at *m/z* 541.2776 $[M+Na]^+$ (calcd for $C_{29}H_{42}NaO_8$, 541.2778), corresponding to a molecular formula $C_{29}H_{42}O_8$. From the ^{1}H and ^{13}C NMR spectra, two acetyloxy groups were apparent. In addition, the carbon signals (δ_C 172.5, 43.7, 25.5, 22.3, and 22.4), together with the corresponding methyl, methylene and methine proton signals (Table 2), disclosed the same isovaleryloxy moiety in compound **2** as that of **1**. The remaining 20 carbons in the ^{13}C NMR spectrum indicated compound **2** to be a diterpenoid [26–29]. Comparison of the chemical shifts of skeletal carbons of **2** with those of compound **1** implied that two compounds shared the same clerodane-type diterpenoid scaffold, which was supported by the following DEPT, HMQC, HMBC, and ^{1}H-^{1}H COSY experiments. The subsequent interpretation of the 2D NMR data led to the assignments of the skeletal proton and carbon signals in compound **2**, and the same skeleton as that of compound **1** was confirmed as depicted in Fig. 2. The HMBC correlations shown in Fig. 2 allowed the isovaleryloxy and acetyloxy groups to be placed at C-6, C-18, and C-19, respectively. There were no other substituent groups in **2**, so a hydroxy group was assigned to C-2 based on the chemical shift of C-2 (δ_C 63.8) and the HRESIMS data. The same relative configuration for compound **2** as that of **1** was corroborated by detailed analysis of the NOESY spectra, where the C-2 hydroxy group, the C-6 isovaleryloxy group, the acetyloxy groups located at C-18 and

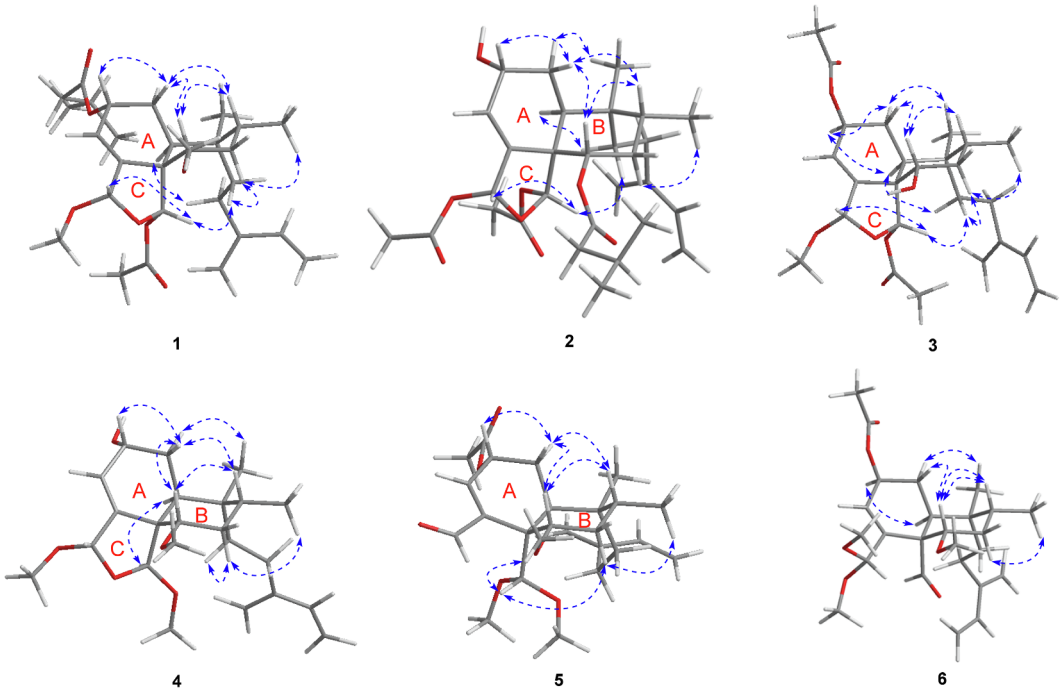

Fig. 3. Conformations and key NOESY correlations of compounds **1–6**.

C-19 were assigned as all *α*-oriented. After elucidating the relative configuration, the absolute configuration of **2** was established by the TDDFT ECD calculations as used for compound **1**. The calculated ECD spectrum matched the experimental data closely (Fig. 4B), leading to the assignment of a (2*R*, 5*S*, 6*S*, 8*R*, 9*R*, 10*S*, 18*R*, 19*S*) absolute configuration for compound **2**. Hence, the structure of **2** was characterized and named kurzipene B.

Compound **3** possessed a molecular formula $C_{25}H_{36}O_7$ based on the presence of a HRESIMS ion peak at *m/z* 471.2358 $[M+Na]^+$ (calcd for $C_{25}H_{36}NaO_7$, 471.2359) and its ^{13}C NMR data. The ^1H and ^{13}C NMR spectra indicated compound **3** to have the same clerodane diterpenoid skeleton as those of compounds **1** and **2** and possess one methoxy and two acetyloxy groups [30–33]. This deduction was concluded by interpretation of the HMQC, HMBC, and ^1H-^1H COSY data. Following the skeleton confirmation and the assignments of skeletal proton and carbon signals, the placements of substituent groups were accomplished by the cross-peaks in the HMBC spectrum. The two acetyloxy groups were found to be located at C-2 and C-19 by the long-range couplings of H-2 and H-19 to the carbonyl carbons of two acteyloxy groups, and the methoxy group was located at C-18 by the HMBC correlations of H-18 to the methoxy carbon and the methoxy protons to C-18. Due to no other substituent groups in **3**, a hydroxy group was inferred to be attached at C-6, which was supported by the NMR and HRESIMS data.

A NOESY spectrum and Chem3D modeling revealed a similar molecular conformation to that of compound **2**, and the only configurational difference is the change of H-2 from a *β*-orientation in **2** to an *α*-orientation in **3**, which was supported by the coupling constants (compound **2**, $J_{2,1\alpha/1\beta} = \sim 0$ Hz; compound **3**, $J_{2,1\alpha/1\beta} = 8.3$ Hz) and NOESY correlations as shown in Fig. 3. The absolute configuration of **3** was determined as 2*S*, 5*S*, 6*S*, 8*R*, 9*R*, 10*S*, 18*S*, and 19*S* by comparison of its experimental and calculated ECD spectra (Fig. 4C). Compound **3** was therefore elucidated and named kurzipene C.

The molecular formula of compound **4** was determined as $C_{23}H_{36}O_5$ based on the HRESIMS (*m/z* 415.2460 $[M+Na]^+$, calcd for $C_{23}H_{36}NaO_5$, 415.2460). From the ^1H and ^{13}C NMR spectra, no acyloxy groups, but three methoxy moieties were deduced affirmatively. The remaining proton and carbon signals revealed compound **4** to have the same framework as those of compounds **1–3**, which was verified by 2D NMR experiments [34–36]. Analysis of the 2D NMR data resulted in the assignments of proton and carbon signals and the placements of three methoxy groups located at C-6, C-18, and C-19. NOESY interactions and Chem3D modeling (Fig. 3) revealed the same skeleton conformation for **4** as those of compounds **1** and **2** and enabled the C-2 hydroxy group and the methoxy groups located at C-6, C-18, and C-19 to be determined as *α*-, *α*-, *α*-, and *β*-oriented, respectively. The absolute configuration of **4** was assigned to be 2*R*, 5*S*, 6*S*, 8*R*, 9*R*, 10*S*, 18*S*, and 19*S*, via comparison of experimental and calculated ECD spectra (Fig. 4D), of which the latter was obtained using the TDDFT method. Compound **4** was therefore elucidated and given a trivial name kurzipene D.

Compound **5** was obtained as a colorless oil. It gave the molecular formula $C_{25}H_{38}O_6$ as determined from the HRESIMS (*m/z* 457.2562 $[M+Na]^+$, calcd for $C_{25}H_{38}NaO_6$, 457.2566). The ^1H and ^{13}C NMR spectra revealed the presence of one acetyloxy group and three methoxy groups based on the substituent groups present in compounds **1–4**. The remaining 20 carbon resonances occurred in the ^{13}C NMR spectrum indicated a diterpenoid skeleton for **5** [37,38]. Comparison of ^{13}C NMR data of the skeleton of **5** with those of compounds **1–4** disclosed that one of acetal carbon signal in **1–4** was replaced by an aldehyde carbon (δ_C 201.7), which implied the cleavage of the furan ring C. The following 2D NMR experiments substantiated the above deductions, and the acetyloxy and three methoxy groups were assigned to C-2, C-6, C-19, and C-19, respectively, via interpretation of the 2D NMR data. A NOESY experiment permitted the relative configuration of **5** to be assigned, displaying the interactions of H-1*β*/H-8, H-8/H-6, H-1*β*/H-6, H-19/H_2-11, H-19/H-7*α*, H-7*α*/H_2-11, H-7*α*/H_3-17, H-10/H_2-11, and H-1*α*/H_3-20 (Fig. 3). These NOE effects, together with Chem3D modeling, suggested the *cis*-fusion of two six-membered rings with H-10 and C-19 both on the *α*-side. Consequently, the C-2 acetyloxy group and the C-6 methoxy group were determined as both *α*-oriented, which were also supported by the coupling constants between H-2/H_2-1 ($J_{2,1\alpha/1\beta} = 4.3$ Hz) and H-6/H_2-7 ($J_{6,7\alpha/7\beta} = 12.6$, 4.3 Hz). ECD calculations and comparison of experimental and calculated ECD spectra (Fig. 4E) allowed the absolute configuration of **5** to be assigned as 2*R*, 5*S*, 6*S*, 8*R*, 9*R*, and 10*S*. Compound **5** was therefore elucidated and given a trivial name kurzipene E.

The HRESIMS suggested that compound **6** had the same molecular

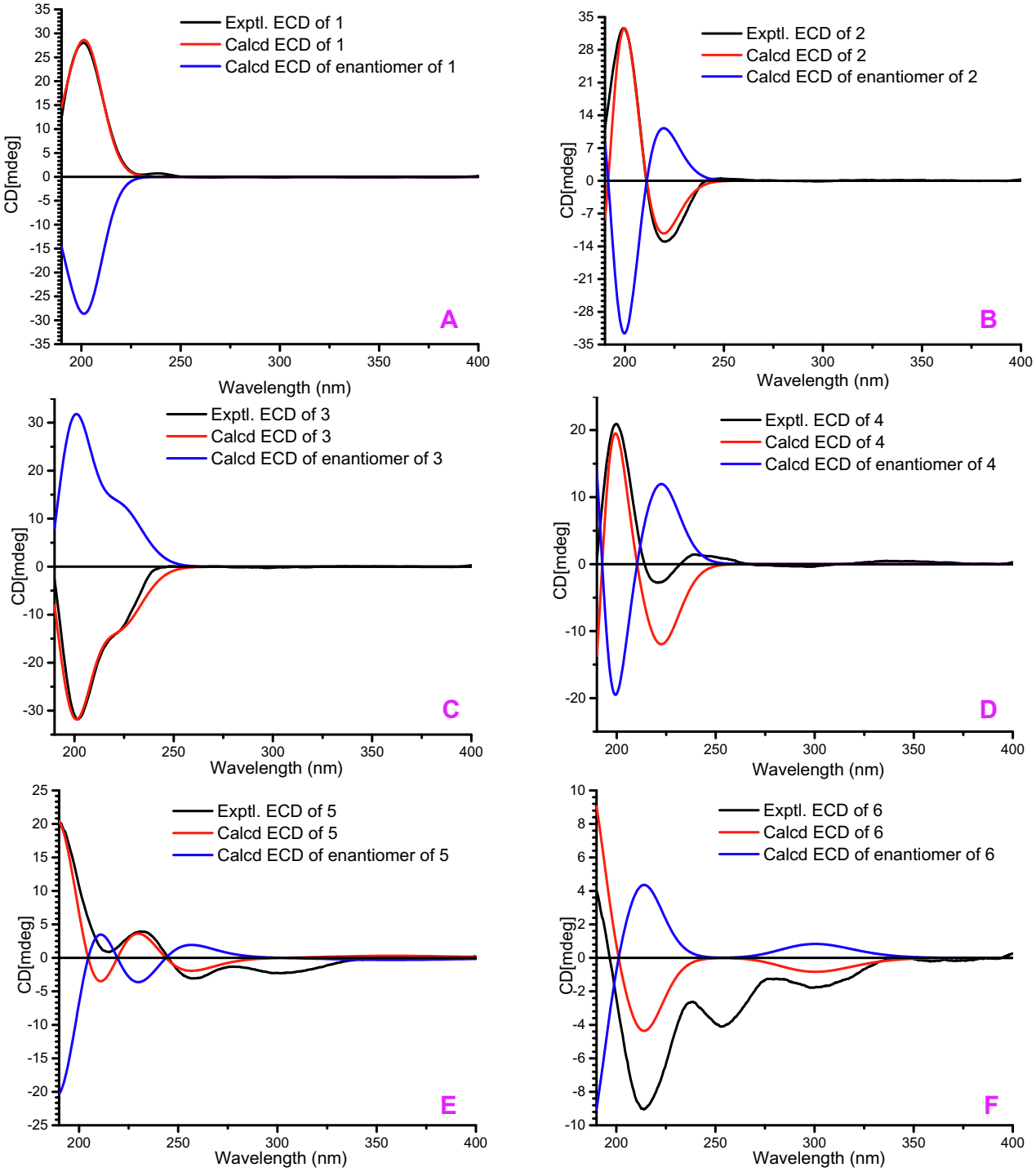

Fig. 4. Calculated and experimental ECD spectra of compounds **1–6** in acetonitrile.

formula $C_{25}H_{38}O_6$ as compound **5**, as supported by the ^{13}C NMR data. From the ^{1}H and ^{13}C NMR spectra of compound **6**, the same acetyloxy and three methoxy groups as present in compound **5** were obvious. Excluding the signals for the substituent groups, the chemical shifts of 20 skeletal carbons were almost identical to those of compound **5**, suggesting compound **6** possessed a diterpenoid skeleton similar to that of compound **5** [39,40]. To determine the skeleton and locations of these substituent groups, DEPT, HMQC, HMBC, and ^{1}H-^{1}H COSY experiments were conducted. By interpretation of the 2D NMR data, the cleavage of furan ring in compound **6** led to the formation of an aldehyde group at C-19, and the acetyloxy and three methoxy groups attributable to C-2, C-6, C-18, and C-18 were also determined. It was found that the main structural difference between compounds **5** and **6** was that the aldehyde group shifted from C-18 in **5** to C-19 in **6**. In addition, the coupling constants of H-2/H_2-1 ($J_{2,1\alpha/1\beta}$ = 8.6 Hz) and H-6/H_2-7 ($J_{6,7\alpha/7\beta}$ = 11.2, 5.0 Hz) in compound **6** indicated a β-orientaton for the C-2 acetyloxy group and an α-orientaton for the C-6 methoxy group [11,12], which were supported by the NOESY spectrum (Fig. 3). Using the same TDDFT calculations as applied for compounds **1–5**, the calculated spectrum of **6** was obtained. The good agreement of

Table 3
Cytotoxicities of compounds **1–6** against three human cancer cell clines.

Compound	A549 (μM)	Hela (μM)	HepG2 (μM)
1	19.0 ± 0.4	15.8 ± 1.1	> 60
2	8.7 ± 0.9	5.3 ± 0.7	8.1 ± 0.5
3	44.4 ± 2.7	28.8 ± 2.6	32.3 ± 1.5
4	> 60	> 60	> 60
5	> 60	> 60	> 60
6	> 60	> 60	> 60
Etoposide[a]	12.5 ± 1.3	36.1 ± 5.2	2.5 ± 0.3

[a] Etoposide was used as a positive control. All results are expressed as the mean ± SD.

experimental and calculated data (Fig. 4F) suggested a (2*S*,5*S*,6*S*,8*R*,9*R*,10*S*) absolute configuration for **6**. Compound **6** was therefore elucidated and given a trivial name kurzipene F.

3.2. Cytotoxic activities

Cancer is a serious and huge threat to human health and has been concerned extensively by the public. It is therefore an urgent need to develop new agents to treat cancer effectively. Related studies have shown that the discovery of bioactive natural products plays an important role in the research and development of new agents to treat cancer [41,42]. To obtain bioactive natural products as lead compounds for cancer, compounds **1–6** isolated from the leaves of *C. kurzii* were evaluated for their cytotoxic activities against three cell lines A549, Hela, and HepG2 cells using a protocol reported previously [43,44]. Etoposide was used as a positive control [45]. All of the compounds exhibited cytotoxic effects toward three cancer cell lines. For human lung cancer A549 cells, compounds **4–6** showed weak activities with IC_{50} values more than 60 μM, compound **3** exhibited moderate effects with IC_{50} value of 44.4 μM, and compounds **1** and **2** showed strong cytotoxic effects with IC_{50} values of 19.0 and 8.7 μM, respectively. The IC_{50} values of compounds **1** and **2** cytotoxic to A549 cells were less than 20 μM and comparable to the positive control etoposide (IC_{50} value, 12.5 μM). For human cervical cancer Hela cells, compounds **4–6** were weakly effective (IC_{50} values > 60 μM), and compounds **1–3** showed promising activities with IC_{50} values less than 30 μM compared to the positive control etoposide (IC_{50} value, 36.1 μM). For human hepatocellular carcinoma HepG2 cells, compounds **2** and **3** possessed strong cytotoxicities with IC_{50} values of 8.1 and 32.3 μM, respectively, while the other compounds were weakly cytotoxic (IC_{50} values > 60 μM). These cytotoxic data were collated in Table 3, which revealed that compound **2** was the most active toward three cancer cell lines.

3.3. Apoptosis effects induced by compound 2

All of the compounds were cytotoxic toward three cancer cell lines and compound **2** seemed to be the most active, especially to Hela cells. To understand the possible action mechanism of cytotoxicity, compound **2**, the most potent compound, was selected to investigate the apoptosis effects on Hela cells. The cells were treated with different concentrations (2.7, 8, and 24 μM) of compound **2** for 48 h, and then the cells were harvested, stained with Annexin V and propidium iodide (PI), and subsequently analyzed by flow cytometry. As shown in Fig. 5, significant apoptotic effects on Hela cells induced by compound **2** were observed clearly. With the increase of concentration of compound **2**, the percentage of apoptotic cells rose from 5.83% (2.7 μM) to 23.43% (8 μM) and 93.50% (24 μM). The data indicated that compound **2** induced apoptosis of Hela cells in a dose-dependent manner (see Fig. 5).

3.4. Effects of compound 2 on cell cycle

Apoptosis, or programmed cell death, is intimately coupled to cell cycle progression, which means interruption or arrest of cell cycle [46]. Cell cycle includes generally interphase (G1, S, and G2 phases) and mitosis phase (M phase). Therefore, to better understand cytotoxic mechanism, the effects of compound **2** on the cell cycle distribution of Hela cells were evaluated. To understand the apoptosis process of Hela cells induced by compound **2**, cell cycle distribution was evaluated

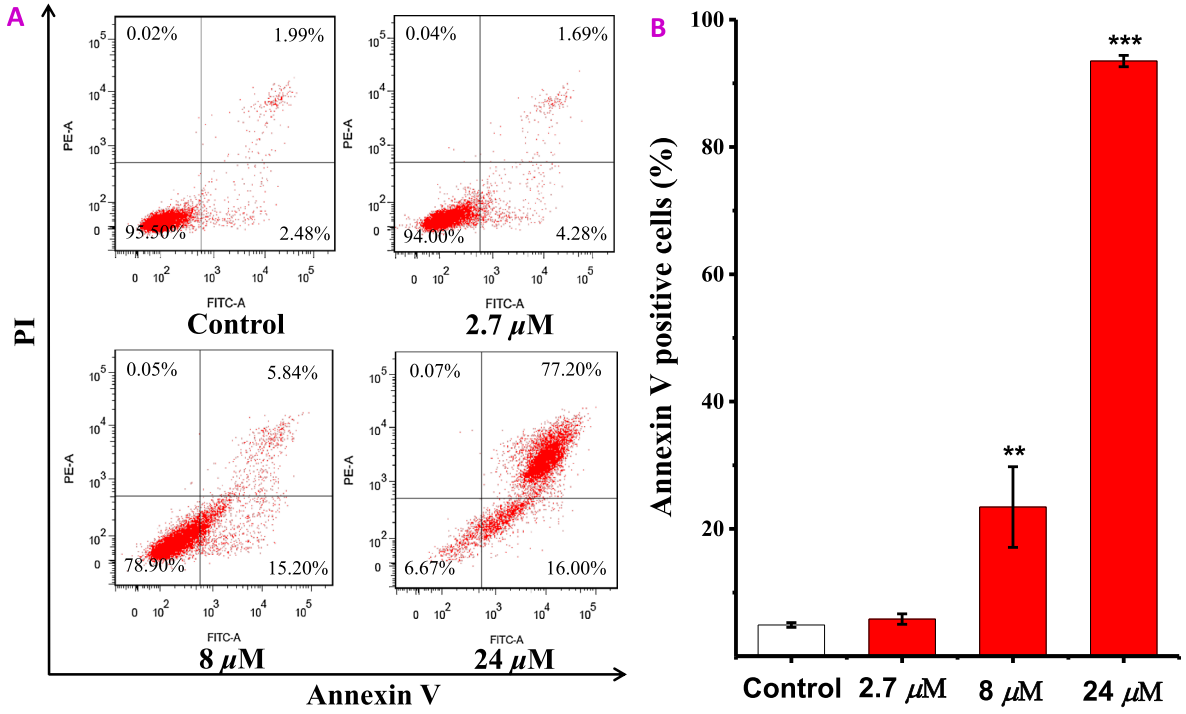

Fig. 5. Apoptosis effects of Hela cells induced by compound 2. Hela cells were treated with different concentrations (2.7, 8, and 24 μM) of compound **2** for 48 h. Then the cells were harvested, stained with Annexin V and propidium iodide (PI), and subsequently analyzed by flow cytometry. (A) Flow cytometric analysis of Hela cells treated with different concentrations of compound **2**. (B) Histogram of apoptotic cells at 48 h with the treatment of compound **2**. (**) $p < 0.01$, (***) $p < 0.001$.

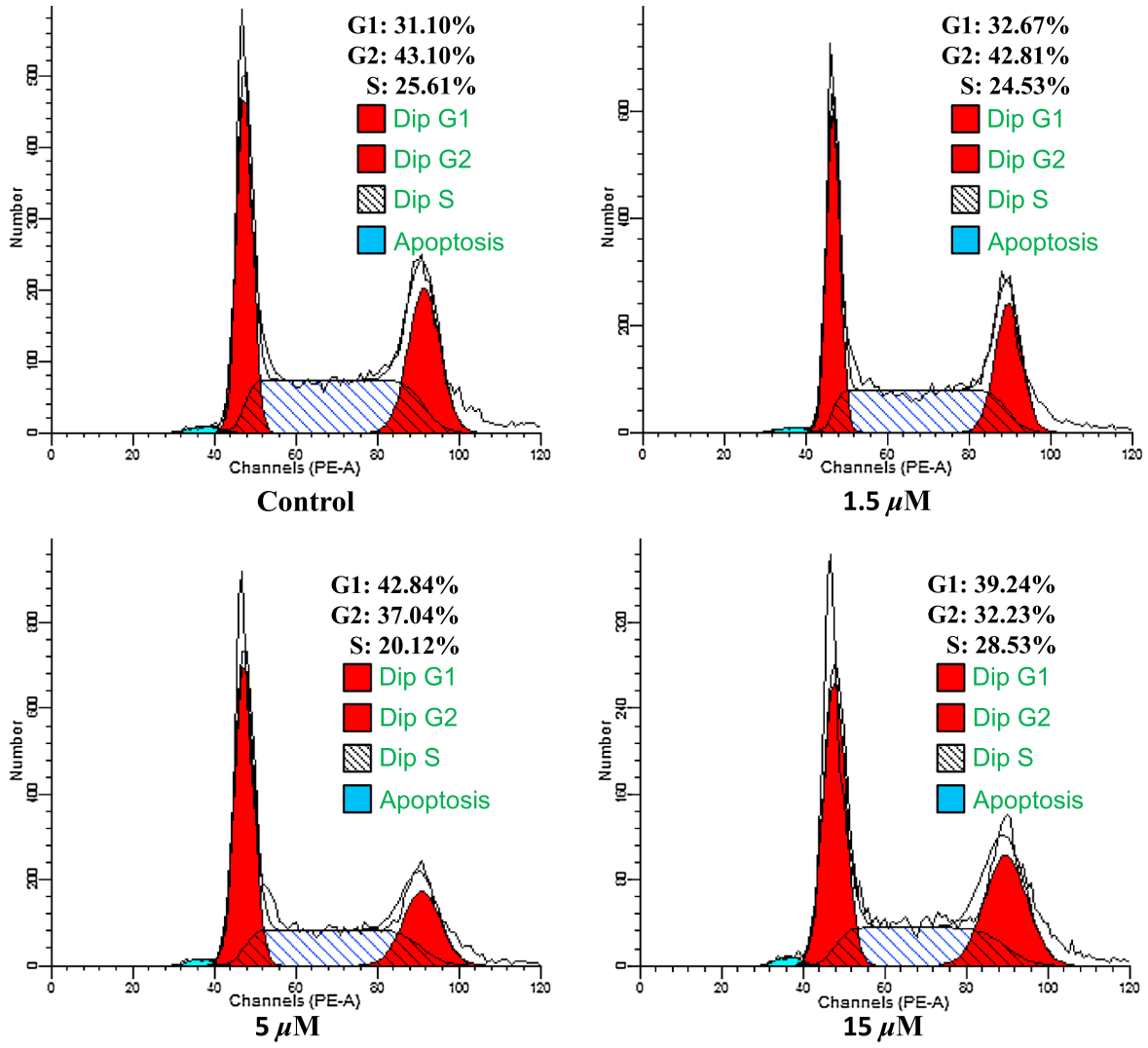

Fig. 6. Arrest effects of **2** on Hela cell cycle. Hela cells were treated with different concentrations (1.5, 5, and 15 μM) of compound **2** for 48 h. Then the cells were harvested and stained with propidium iodide (PI), and the cell cycle distribution was analyzed using flow cytometry.

using flow cytometric analysis. After treated with different concentrations (1.5, 5, and 15 μM) of compound **2** for 48 h, the cell proportion in different phases varied following the change of concentrations. Compared to the control, the percentages of the cells in the G0/G1 phase increased markedly and the cells in G2/M phase decreased when treated with the concentration of 15 μM of compound **2** (Fig. 6). These data suggested that compound **2** arrested the Hela cell cycle at the G0/G1 stage, leading to the cell apoptosis.

4. Conclusion

The present phytochemical investigation on the leaves of *C. kurzii* has led to the isolation of six new clerodane diterpenoids, kurzipenes A–F (**1–6**). Their structures were elucidated on the basis of 1D and 2D NMR spectroscopic data analysis, and the absolute configurations of compounds **1–6** were established via comparison of experimental and calculated ECD spectra. All of the compounds were evaluated for their cytotoxic activities toward A549, Hela, and HepG2 cells. Most diterpenoids showed potent cytotoxicities against the selected cancer cells. Compound **2** showed most potent cytotoxic effects against Hela cells with an IC_{50} value of 5.3 μM. The preliminary mechanism studies revealed that compound **2** induced apoptosis and arrested the Hela cell cycle at the G0/G1 stage to exert cytotoxic effects.

Conflict of interest

The authors of the present manuscript have declared that no competing interests exist.

Acknowledgments

This work was supported by the National Key Research and Development Program of China (No. 2018YFA0507204), the National Natural Science Foundation of China (Nos. U1703107, 21642016, and 21372125), the Natural Science Foundation of Tianjin, China (No. 16JCYBJC27700), Hundred Young Academic Leaders Program of Nankai University, State Key Laboratory for Chemistry and Molecular Engineering of Medicinal Resources (Guangxi Normal University, No. CMEMR2018-B02), and the Fundamental Research Funds for the Central Universities.

Appendix A. Supplementary material

Supplementary data to this article can be found online at https://doi.org/10.1016/j.bioorg.2019.01.048.

References

[1] D.J. Newman, G.M. Cragg, J. Nat. Prod. 79 (2016) 629–661.
[2] Editorial Committee of the Flora of China, Chinese Academy of Sciences. Flora of China, vol. 52(1), Science Press, Beijing, 1999, pp. 69−71.
[3] L. Xia, Q. Guo, P. Tu, X. Chai, Phytochem. Rev. 14 (2015) 99–135.
[4] A.L. Santos, E.S. Yamamoto, L.F.D. Passero, M.D. Laurenti, L.F. Martins, M.L. Lima, M. Uemi, M.G. Soares, J.H.G. Lago, A.G. Tempone, P. Sartorelli, Chem. Biodivers. 14 (2017) e1600458.
[5] A.P. Piovezan, A.P. Batisti, M.L.A.C.S. Benevides, B.L. Turnes, D.F. Martins, L. Kanis, E.C.W. Duarte, A.J. Cavalheiro, P.C.P. Bueno, M.P. Seed, L.V. Norling, D. Cooper, S. Headland, P.R.P.S. Souza, M. Perretti, J. Ethnopharmacol. 204 (2017) 179–188.
[6] É.J. Ferreira de Araújo, A.A. Cardoso de Almeida, O.A. Silva, I.H. Fernandes da Costa, L.M. Rezende-Júnior, F.C.A. Lima, A.J. Cavalheiro, C. Pessoa, M. Odorico de Moraes, P.M.P. Ferreira, J. Ethnopharmacol. 198 (2017) 460–467.
[7] P.M.P. Ferreira, D.P. Bezerra, J.N. Silva, M. Pinheiro da Costa, J.R. Ferreira, N.M.N. Alencar, I.S. Tavares de Figueiredo, A.J. Cavalheiro, C.M.L. Machado, R. Chammas, A.P.N.N. Alves, M. Odorico de Moraes, C. Pessoa, J. Ethnopharmacol. 186 (2016) 270–279.
[8] R. Moreira da Silva, S. Verjee, C.M. de Gaitani, A.R. Moraes de Oliveira, P.C. Pires Bueno, A.J. Cavalheiro, N. Peporine Lopes, V. Butterweck, J. Nat. Prod. 79 (2016) 1084–1090.
[9] J. Xu, J. Kang, X. Sun, X. Cao, K. Rena, D. Lee, Q. Ren, S. Li, Y. Ohizumi, Y. Guo, J. Nat. Prod. 79 (2016) 170–179.
[10] J. Xu, Q. Zhang, M. Wang, Q. Ren, Y. Sun, D.Q. Jin, C. Xie, H. Chen, Y. Ohizumi, Y. Guo, J. Nat. Prod. 77 (2014) 2182–2189.
[11] J. Xu, F. Ji, X. Sun, X. Cao, S. Li, Y. Ohizumi, Y. Guo, J. Nat. Prod. 78 (2015) 2648–2656.
[12] Md.S.H. Khan, Md.F. Molla, S. Sultana, S. Rahman, M. Rahmatullah, J. Chem. Pharm. Res. 7 (2015) 420–424.
[13] P.M.P. Ferreira, G.C.G. Militao, D.J.B. Lima, N.D.J. Costa, K.C. Machado, A.G. Santos, A.J. Cavalheiro, V.S. Bolzani, D.H.S. Silva, C. Pessoa, Chem. Biol. Interact. 222 (2014) 112–125.
[14] H.T. Nguyen, N.B. Truong, H.T. Doan, M. Litaudon, P. Retailleau, T.T. Do, H.V. Nguyen, M.V. Chau, C.V. Pham, J. Nat. Prod. 78 (2015) 2726–2730.
[15] D.D. Bou, A.G. Tempone, E.G. Pinto, J.H.G. Lago, P. Sartorelli, Phytomedicine 21 (2014) 676–681.
[16] F. Liu, X. Yang, J. Ma, Y. Yang, C. Xie, M. Tuerhong, D.Q. Jin, J. Xu, D. Lee, Y. Ohizumi, Y. Guo, Bioorg. Chem. 75 (2017) 149–156.
[17] J. Xu, M. Wang, X. Sun, Q. Ren, X. Cao, S. Li, G. Su, M. Tuerhong, D. Lee, Y. Ohizumi, M. Bartlam, Y. Guo, J. Nat. Prod. 79 (2016) 2924–2932.
[18] P. Wang, X. Yang, F. Liu, Y. Liang, G. Su, M. Tuerhong, D.Q. Jin, J. Xu, D. Lee, Y. Ohizumi, Y. Guo, Bioorg. Chem. 76 (2018) 53–60.
[19] X. Cao, X. Yang, P. Wang, Y. Liang, F. Liu, M. Tuerhong, D.Q. Jin, J. Xu, D. Lee, Y. Ohizumi, Y. Guo, Bioorg. Chem. 75 (2017) 139–148.
[20] M.J. Frisch, G.W. Trucks, H.B. Schlegel, G.E. Scuseria, M.A. Robb, J.R. Cheeseman, G. Scalmani, V. Barone, B. Mennucci, G.A. Petersson, H. Nakatsuji, M. Caricato, X. Li, H.P. Hratchian, A.F. Izmaylov, J. Bloino, G. Zheng, J.L. Sonnenberg, M. Hada, M. Ehara, K. Toyota, R. Fukuda, J. Hasegawa, M. Ishida, T. Nakajima, Y. Honda, O. Kitao, H. Nakai, T. Vreven, J.A. Montgomery Jr., J.E. Peralta, F. Ogliaro, M. Bearpark, J.J. Heyd, E. Brothers, K.N. Kudin, V.N. Staroverov, R. Kobayashi, J. Normand, K. Raghavachari, A. Rendell, J.C. Burant, S.S. Iyengar, J. Tomasi, M. Cossi, N. Rega, J.M. Millam, M. Klene, J.E. Knox, J.B. Cross, V. Bakken, C. Adamo, J. Jaramillo, R. Gomperts, R.E. Stratmann, O. Yazyev, A.J. Austin, R. Cammi, C. Pomelli, J.W. Ochterski, R.L. Martin, K. Morokuma, V.G. Zakrzewski, G.A. Voth, P. Salvador, J.J. Dannenberg, S. Dapprich, A.D. Daniels, O. Farkas, J.B. Foresman, J.V. Ortiz, J. Cioslowski, D.J. Fox, Gaussian 09, Revision A.02, Gaussian Inc, Wallingford, CT, 2009.
[21] T. Bruhn, A. Schaumlöffel, Y. Hemberger, G. Bringmann, SpecDis, Version 1.62, University of Wuerzburg, Germany, 2014.
[22] B. Wang, X.L. Wang, S.Q. Wang, T. Shen, Y.Q. Liu, H. Yuan, H.X. Lou, X.N. Wang, J. Nat. Prod. 76 (2013) 1573–1579.
[23] G.M. Vieira-Júnior, L.A. Dutra, P.M. Ferreira, M.O. de Moraes, L.V. Costa Lotufo, C.Ó. Pessoa, R.B. Torres, N. Boralle, V.S. Bolzani, A.J. Cavalheiro, J. Nat. Prod. 74 (2011) 776–781.
[24] W. Wang, J. Zhao, Y.H. Wang, T.A. Smillie, X.C. Li, I.A. Khan, Planta Med. 75 (2009) 1436–1441.
[25] E.L. Whitson, C.L. Thomas, C.J. Henrich, T.J. Sayers, J.B. McMahon, T.C. McKee, J. Nat. Prod. 73 (2010) 2013–2018.
[26] T.B. Chen, D.F. Wiemer, J. Nat. Prod. 54 (1991) 1612–1618.
[27] P.M.P. Ferreira, A.G. Santos, A.G. Tininis, P.M. Costa, A.J. Cavalheiro, V.S. Bolzani, M.O. Moraes, L.V. Costa-Lotufo, R.C. Montenegro, C. Pessoa, Chem. Biol. Interact. 188 (2010) 497–504.
[28] W. Wang, Z. Ali, X.C. Li, I.A. Khan, Helv. Chim. Acta 92 (2009) 1829–1839.
[29] G.M. Vieira-Junior, T.O. Goncalves, L.O. Regasini, P.M.P. Ferreira, C.O. Pessoa, L.V. Costa-Lotufo, R.B. Torres, N. Boralle, V.S. Bolzani, A.J. Cavalheiro, J. Nat. Prod. 72 (2009) 1847–1850.
[30] W. Wang, Z. Ali, X.C. Li, T.A. Smillie, D.A. Guo, I.A. Khan, Fitoterapia 80 (2009) 404–407.
[31] S. Gibbons, A.I. Gray, P.G. Waterman, Phytochemistry 41 (1996) 565–570.
[32] S. Kanokmedhakul, K. Kanokmedhakul, M. Buayairaksa, J. Nat. Prod. 70 (2007) 1122–1126.
[33] R.B. Williams, A. Norris, J.S. Miller, C. Birkinshaw, F. Ratovoson, R. Andriantsiferana, V.E. Rasamison, D.G.I. Kingston, J. Nat. Prod. 70 (2007) 206–209.
[34] C.V.S. Prakash, J.M. Hoch, D.G.I. Kingston, J. Nat. Prod. 65 (2002) 100–107.
[35] S. Kanokmedhakul, K. Kanokmedhakul, T. Kanarsa, M. Buayairaksa, J. Nat. Prod. 68 (2005) 183–188.
[36] M.S. Hunter, D.G. Corley, C.P. Carron, E. Rowold, B.F. Kilpatrick, R.C. Durley, J. Nat. Prod. 60 (1997) 894–899.
[37] N.H. Oberlies, J.P. Burgess, H.A. Navarro, R.E. Pinos, C.R. Fairchild, R.W. Peterson, D.D. Soejarto, N.R. Farnsworth, A.D. Kinghorn, M.C. Wani, M.E. Wall, J. Nat. Prod. 65 (2002) 95–99.
[38] J.A. Beutler, K.L. McCall, K. Herbert, D.L. Herald, G.R. Pettit, T. Johnson, R.H. Shoemaker, M.R. Boyd, J. Nat. Prod. 63 (2000) 657–661.
[39] P.R.F. Carvalho, M. Furlan, M.C.M. Young, D.G.I. Kingston, V.S. Bolzani, Phytochemistry 49 (1998) 1659–1662.
[40] Y.C. Shen, C.H. Wang, Y.B. Cheng, L.T. Wang, J.H. Guh, C.T. Chien, A.T. Khalil, J. Nat. Prod. 67 (2004) 316–321.
[41] S. Gao, D. Sun, G. Wang, J. Zhang, Y. Jiang, G. Li, K. Zhang, L. Wang, J. Huang, L. Chen, Bioorg. Chem. 69 (2016) 121–128.
[42] J.S. Yu, D. Lee, S.R. Lee, J.W. Lee, C.I. Choi, T.S. Jang, K.S. Kang, K.H. Kim, Bioorg. Chem. 76 (2018) 28–36.
[43] G.D. Yao, Q. Sun, X.Y. Song, X.X. Huang, Y. Zhang, S.J. Song, Bioorg. Chem. 77 (2018) 619–624.
[44] D.H. Li, J.Y. Li, C.M. Xue, T. Han, C.M. Sai, K.B. Wang, J.C. Lu, Y.K. Jing, H.M. Hua, Z.L. Li, J. Nat. Prod. 80 (2017) 2893–2904.
[45] H. Mirzaei, M. Shokrzadeh, M. Modanloo, A. Ziar, G.H. Riazi, S. Emami, Bioorg. Chem. 75 (2017) 86–98.
[46] K.L. King, J.A. Cidlowski, Annu. Rev. Physiol. 60 (1998) 601–617.